2021 43rd Annual International Conference of the
IEEE Engineering in Medicine & Biology Society (EMBC)
Oct 31 - Nov 4, 2021. Virtual Conference

A 3-DOF Bionic Waist Joint for Humanoid Robot*

Yiwei Wang, Wenyang Li, *Member, IEEE,* Tongyang Cao, Shunta Togo, Hiroshi Yokoi, *Member, IEEE, and Yinlai Jiang, Member, IEEE*

***Abstract*—In this study, a 3 degree-of-freedom bionic waist joint was developed with coupled tendon-driven mechanism. This bionic waist joint can not only ensure the safety of the human-robot interface, but also increase the load capacity without increasing the weight. The coupled tendon-driven mechanism enables the motion of each joint to be driven by at least two motors together, and enables a maximum torque of 3 times the maximum motor output torque at each joint. The bionic waist joint has similar kinematic characteristics to a human waist, including degrees of freedom (DOF) and range of motion (ROM). The problem of coexistence of coupling and decoupling in the same rotating joint was solved with a novel mechanism that can promote further versatility of the coupled tendon-driven mechanism. The basic movements and characteristics of the waist was validated in the experiment.**

I. Introduction

Humanoid robots have been attracting attention in recent years due to the high demand for robots that can interact with people. In Japan, the population of elderly people aged 65 years or older was 26.6% of the total population in 2015 [1]. In the United States, there is an estimated incidence of tetraplegia or paraplegia of 230 000 persons a year [2]. The replacement of upper limb functions is expected to dramatically improve the quality of life (QOF) of patients. In order to mimic the movements of the human body and to realize complex tasks that can be performed by humans, multi-degree-of-freedom (multi-DOF) joints are necessary.

Power transmission via wires (tendons) has been used in robotic hands [3], and robotic arms [4]. Compared to other transmission devices, the wires are lighter, do not require a lot of space, and offer more flexibility in positioning the motor. In addition, the physical properties of the wire are useful in mimicking the inherent compliance and dynamics characteristics. The flexibility of the tendon improves the safety of the robot in its physical interaction with humans [5].

There are currently two types of robot torso parts: the first is a rigid type with no degree-of-freedom (DOF), and the second is a torso with 2- or 3-DOF movable waist joints. The WABIAN-2 LL robot [6] has a 2-DOF waist and a 2-DOF trunk, and the trunk is designed to rotate in combination with the 2-DOF waist. The waist of the LIMS2-AMBIDEX robot [7] have three DOFs and can lift a load of up to 23 kg due to an additional gravity compensation mechanism in the waist joint. The iCub robot [8] was designed with a 3-DOF tendon-driven differential waist joint. The addition of the waist joint tends to increase the complexity of the robot structure, but it also improves the robot's range of motion (ROM) and increase interactivity with human.

In this study, we proposed a coupled tendon-driven mechanism to develop a compact and high-power bionic waist joint. There are at least two motors working simultaneously during the movement of each joint due to the coupled structure. In addition, the coexistence of coupled and decoupled in the same rotational joint is clarified and solved with a novel mechanism, which leads to further versatility of the coupled tendon-driven mechanism.

Section II analyzes the 3-motor 3-degree-of-freedom (3M3D) coupled tendon-driven mechanism, along with the corresponding torque formula and rotation angle formula, and the appropriate structure is selected for the bionic waist joint in this study. Section III describes the detail design of the bionic waist joint, while presenting a wire adjustment mechanism used for joint decoupling. Section IV presents the validation experiment of the bionic waist joint. And the final section shows the conclusion and discusses the future work.

II. 3M3D Coupled Tendon-Driven Joint Module

A. 3M3D Coupled Tendon-Driven Mechanism

In a general uncoupled tendon-driven mechanism, when a single joint is rotating, there is only one motor in working state and the other motors are in standby, which is a waste of resources for the whole mechanism. If we can realize the coupled tendon-driven in which one joint driven by multiple motors together, a larger joint torque is available by reasonably allocating the motor resources. Li et al. [9] proposed four possible 3-motor 3-DOF (3M3D) coupled tendon-driven mechanisms (a. full routing structure, b. 1-skipped routing structure, c. 2-skipped routing structure, and d. 3-skipped routing structure).

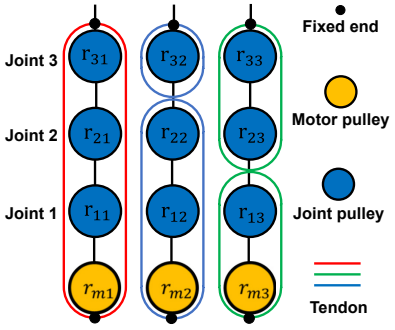

Figure 1. The full routing structure of 3M3D mechanism.

The full routing structure is shown in Fig.1. Here, r_{mj} (j represents the wire path where the motor j is located, j = 1, 2,

*This research was supported in part by JSPS KAKENHI grant numbers JP18H03761, JP19K14941, JP19K12877, and 20J14065.

Y. Wang, W. Li, T. Cao, S. Togo and H. Yokoi are with the Department of Mechanical Engineering and Intelligent Systems, the University of Electro-Communications, Tokyo, 182-8585 Japan. (e-mail: y.wang; li; caotongyang; togo; yokoi@hi.mce.uec.ac.jp).

Y. Jiang is with the Center for Neuroscience and Biomedical Engineering, the University of Electro-Communications, Tokyo, 182-8585 Japan. (phone: 81-42-443-5424; fax: 81-42-443-5913; e-mail: jiang @hi.mce.uec.ac.jp).

3) and r_{ij} (i represents the joint $i, i = 1,2,3$) are the radius of the pulleys. Here, the total torque on the joint is the sum of the torques transmitted by the three motors. And, the total rotation angle of the motor is the sum of the rotation angles of the 3 joints. Therefore, the relationship between the torque and the rotation angle between the motors and the joints can be described in the form of a matrix as:

$$\begin{bmatrix}\tau_1\\ \tau_2\\ \tau_3\end{bmatrix} = \begin{bmatrix} r_{11}/r_{m1} & r_{12}/r_{m2} & r_{13}/r_{m3} \\ r_{21}/r_{m1} & r_{22}/r_{m2} & -r_{23}/r_{m3} \\ r_{31}/r_{m1} & -r_{32}/r_{m2} & -r_{33}/r_{m3}\end{bmatrix}\begin{bmatrix}T_{m1}\\ T_{m2}\\ T_{m3}\end{bmatrix} \quad (1)$$

$$\begin{bmatrix}\theta_{m1}\\ \theta_{m2}\\ \theta_{m3}\end{bmatrix} = \begin{bmatrix} r_{11}/r_{m1} & r_{21}/r_{m1} & r_{31}/r_{m1} \\ r_{12}/r_{m2} & r_{22}/r_{m2} & -r_{32}/r_{m2} \\ r_{13}/r_{m3} & -r_{23}/r_{m3} & -r_{33}/r_{m3}\end{bmatrix}\begin{bmatrix}\theta_1\\ \theta_2\\ \theta_3\end{bmatrix}. \quad (2)$$

Here, a matrix J is introduced for convenience, as shown in Eq. (3). J is a 3×3 matrix called motor-joint routing matrix that describes the wire routing structure between the motors and the joints.

$$\mathrm{J} = \begin{bmatrix} r_{11}/r_{m1} & r_{12}/r_{m2} & r_{13}/r_{m3} \\ r_{21}/r_{m1} & r_{22}/r_{m2} & -r_{23}/r_{m3} \\ r_{31}/r_{m1} & -r_{32}/r_{m2} & -r_{33}/r_{m3}\end{bmatrix}. \quad (3)$$

Then the torque formula and the rotation angle formula can be simply described as:

$$\tau_i = \mathrm{J}T_{mj} \quad (4)$$

$$\theta_{mj} = \mathrm{J}^T\theta_i. \quad (5)$$

Then when separately driving joint 1 alone, the torque of the remaining two joints should be 0, and the torque formula can be described as (Assuming the maximum torque of the motor is T_m and the radii of all pulleys are equal):

$$T_{mj} = \mathrm{J}^{-1}\tau_i = \begin{bmatrix}1 & 1 & 1\\ 1 & 1 & -1\\ 1 & -1 & -1\end{bmatrix}^{-1}\tau_i \quad (6)$$

$$\begin{bmatrix}T_{m1}\\ T_{m2}\\ T_{m3}\end{bmatrix} = \begin{bmatrix}0.5 & 0 & 0.5\\ 0 & 0.5 & -0.5\\ 0.5 & -0.5 & 0\end{bmatrix}\begin{bmatrix}\tau_1\\ 0\\ 0\end{bmatrix} = \begin{bmatrix}0.5\tau_1\\ 0\\ 0.5\tau_1\end{bmatrix}. \quad (7)$$

Eq. (7) shows that when separately drive joint 1, $\tau_2 = \tau_3 = 0$, $\tau_{1(\max)} = 2T_m$, then $T_{m1} = T_{m3} = T_m$, $T_{m2} = 0$. Similarly, when separately driving joint 2 and joint 3 respectively, the maximum torque of joint 2 and joint 3 is $\tau_{2(\max)} = 2T_m$ and $\tau_{3(\max)} = 2T_m$.

B. Selection of Wire Routing Structure for Waist Joint

Li et al. [9] analyzed the maximum torque of the four routing structure and the results showed that when the number of joint pulleys is reduced, it essentially does not affect the maximum joint torque of separating driving single joint alone, but conversely, reducing the number of joint couplings simplifies the coupling structure. Therefore, a 3-skipped routing structure was adopted for the bionic waist joint in this study, and the specific coupling routing structure is shown in Fig.2.

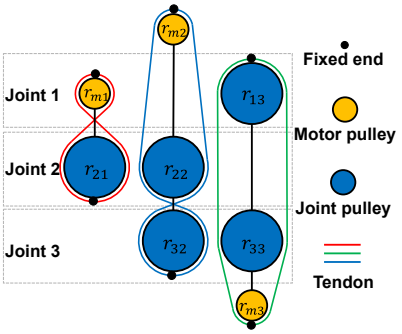

Figure 2. Wire routing and motor location diagram of 3M3D waist joint.

Here, the radius of the joint pulley is twice that of the motor pulley. Therefore, the torque formula and rotation angle formula can be described as:

$$\begin{bmatrix}\tau_1\\ \tau_2\\ \tau_3\end{bmatrix} = \begin{bmatrix}1 & 0 & 2\\ -2 & 2 & 0\\ 0 & -2 & 2\end{bmatrix}\begin{bmatrix}T_{m1}\\ T_{m2}\\ T_{m3}\end{bmatrix} \quad (8)$$

$$\begin{bmatrix}\theta_{m1}\\ \theta_{m2}\\ \theta_{m3}\end{bmatrix} = \begin{bmatrix}1 & -2 & 0\\ 0 & 2 & -2\\ 2 & 0 & 2\end{bmatrix}\begin{bmatrix}\theta_1\\ \theta_2\\ \theta_3\end{bmatrix}. \quad (9)$$

However, there is an unavoidable problem with the 3-skipped routing structure. As shown in the Fig.3, when the three joints are in the position on the figure, for separately driving joint 1, there should be no torque on joint 2 and joint 3. Therefore, how to decouple the tendons from motor 3 to joint 1 at joint 2 is the key problem for realizing 3-skipped routing structure.

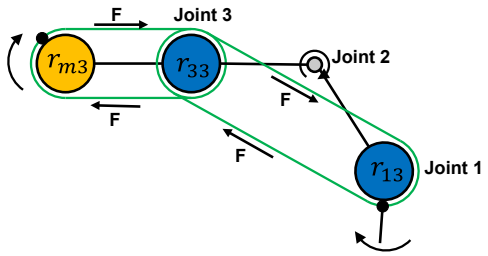

Figure 3. The wire routing structure of the $r_{m3} - r_{33} - r_{13}$.

III. Structural Design

A. Overall Design

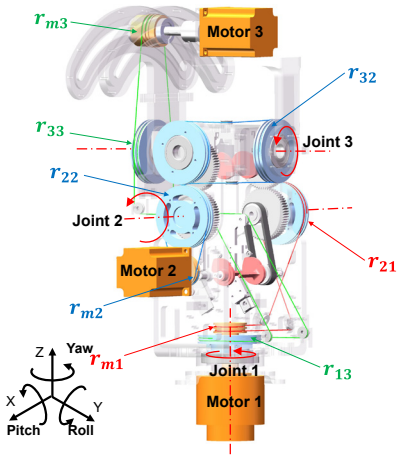

Figure 4. Design of 3M3D coupled tendon-driven waist joint mechanism.

The bionic waist joint structure is shown in Fig.4. The 3M3D coupled tendon-driven with 3-skipped routing structure was adopted as drive method. Fig. 5 shows the wire routing structure of (a) the $r_{m1} - r_{21}$, (b) the $r_{m2} - r_{22} - r_{32}$, and (c) the $r_{m3} - r_{33} - r_{13}$, respectively.

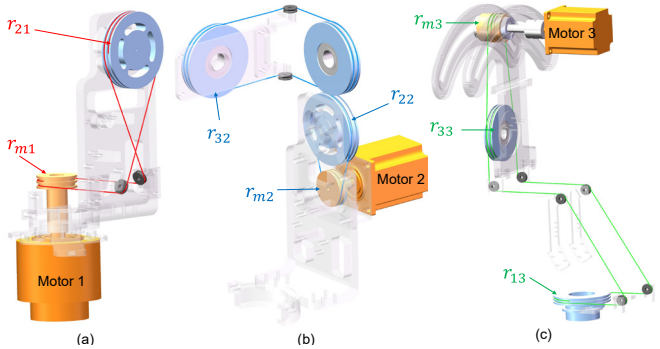

Figure 5. Wire routing structure.

B. *Wire Adjustment Mechanism*

We have previously described that the wire directly connecting joint 1 and joint 3 generates an unwanted torque on joint 2, which affects the motion of the structure. Therefore, decoupling at joint 2 is required. Here, we made the assumption that if the wire connecting joint 1 and joint 3 always passes through the center of rotation (COR) of joint 2, then joint 2 no longer generates a rotational torque.

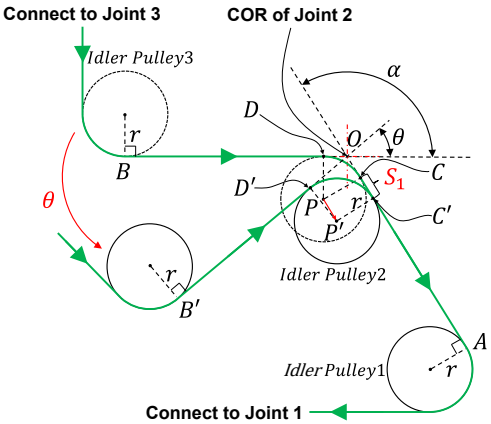

Figure 6. Schematic diagram of decoupling mechanism.

However, when joint 2 is rotated, the position of the idler pulley 2 must be changed in order to meet the above conditionsm, as shown in Fig.6. The relationship between the position difference S_1 and the rotation angle θ is (the radius of the idler pulley is r, initial position: $\angle AOB = \alpha$):

$$S_1 = \overline{OC'} - \overline{OC} = \frac{r}{tan\left(\frac{\alpha-\theta}{2}\right)} - \frac{r}{tan\left(\frac{\alpha}{2}\right)} \quad (10)$$

The change in position of the idler pulley 2 ensures that the wire always passes through the COR of the joint 2. However, due to the change in the position of idler pulley 2, the wire path length between idler pulley 1 and idler pulley 3 changes, which will inevitably cause joint 1 and joint 3 to also rotate during the rotation of joint 2. Therefore, we calculated the relationship between the change in wire path length S_2 and the rotation angle θ, and the results are as follows:

$$\begin{aligned} S_2 &= \overline{AB'} - \overline{AB} = (\overline{OA} + \overline{OB} - \overline{OC} - \overline{OD} + \overline{CD}) \\ &\quad -(\overline{OA} + \overline{OB'} - \overline{OC'} - \overline{OD'} + \overline{C'D'}) \\ &= \frac{2r}{tan\left(\frac{\alpha}{2}\right)} - \frac{2r}{tan\left(\frac{\alpha-\theta}{2}\right)} + \theta r \end{aligned} \quad (11)$$

The adjustment mechanism using cams was developed in this study. As shown in Fig.7, two cams were designed, where the function of cam 1 is to change the position of idler pulley 2. The direction of movement of the guide rail 1 is parallel to the wire 1, which can ensure that the wire 1 always passes the COR of joint 2. The function of cam 2 is to compensate for the wire path length between idler pulley 1 and idler pulley 3. The cam 2 rotates together with the joint 2 to drive the idler pulley 3 in the movement direction of the guide rail 2, thus achieving the compensation of the length.

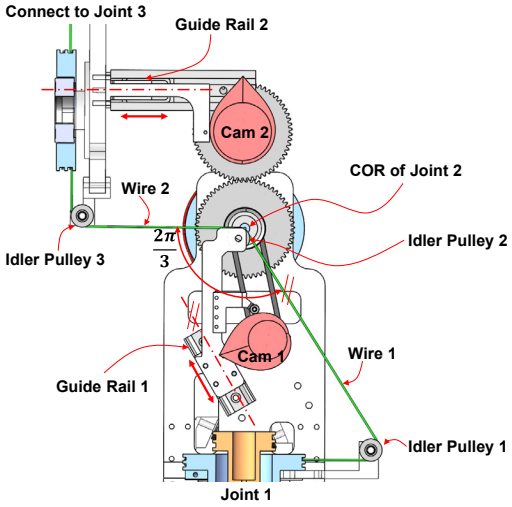

Figure 7. Wire adjustment mechanism.

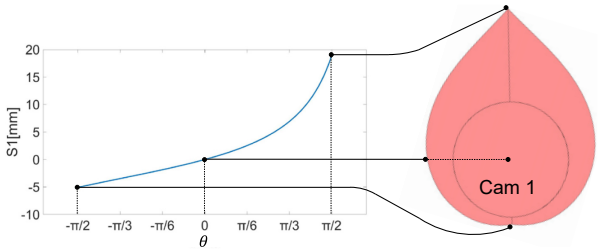

Figure 8. Profile and structure design of cam 1.

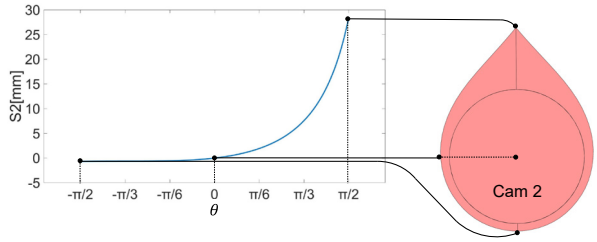

Figure 1. Profile and structure design of cam 2.

According to Eq. (10) and Eq. (11), we first designed the cam profile, and for the cam profile we only considered the part of the joint 2 rotation angle from -90° to 90°, because this angle segment has fully satisfied our joint 2 rotation angle maximum range. We completed the structural design of the two cams separately by means of the cam profile. The specific structures of cams are shown in the Fig.8 and Fig.9.

C. *Specifications of the Bionic Waist Joint*

TABLE I. SPECIFICATIONS OF THE BIONIC WAIST JOINT

Item	*Specifications*
Size (L×W×H) (mm)	335.5×310×535.5
Degrees of Freedom	3
ROM (deg)	-60°~60°(Pitch), -50°~50°(Roll), -90°~90°(Yaw)
No-load speed (rpm)	500(Pitch), 500(Roll), 500(Yaw)
Motor	60AIM25(Motor 1), 57AIM30(Motors 2 and 3)
Wire	SUS304, ϕ0.7 mm (7×19)

The specifications of the bionic waist joint in this study are shown in Table I. The ROM of the bionic waist joint nearly covered the full ROM of a human waist, with the ROM of pitch, roll, and yaw being -30°~80°, -45°~45°, and -35°~35° respectively [10].

IV. PERFORMANCE EVALUATION

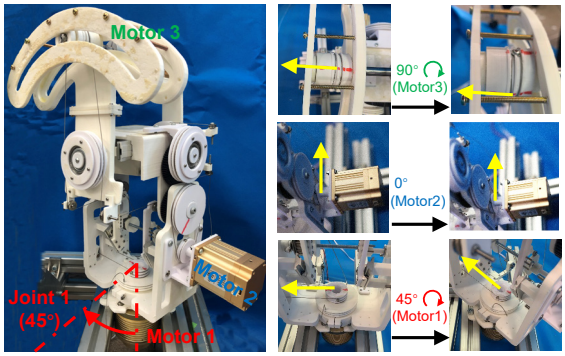

Figure 10. Experiment on the rotation angle of joint 1.

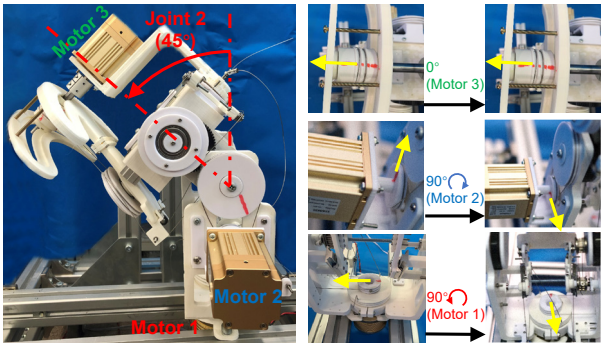

Figure 2. Experiment on the rotation angle of joint 2.

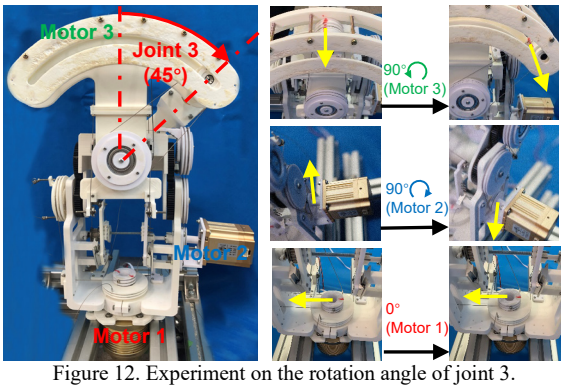

Figure 12. Experiment on the rotation angle of joint 3.

The bionic waist joint adopted a 3M3D coupled tendon-driven mechanism with a 3-skipped routing structure. In order to verify the feasibility of this mechanism, experiments were conducted to verify the effectiveness of the wire adjustment mechanism. Also, to verify the correctness of the rotation angle formula of the coupled tendon-driven mechanism, we tested the relationship between the joint rotation angle and the motor rotation angle.

This verification experiment is to separately rotate one joint by a certain angle (45°), then measure the rotation (angle and direction) of the three motors. The experimental results are shown in Figs.10~12, which demonstrate the correspondence between the rotation angle and direction of the joint and the motor. This result is consistent with the previously theoretically derived rotation angle formula, which proves the correctness of the structure, and also shows that the wire adjustment mechanism produces a role in this structure and the validity is proven.

V. CONCLUSION

In this paper, 3M3D coupled tendon-driven mechanisms are analyzed and studied. Through the analysis and comparison, the 3-skipped routing structure was selected for the bionic waist joint in this study. Based on the designed pulley radius and wire routing, the torque formula and rotation angle formula of this waist joint were derived. In order to solve the over-coupling problem of the 3-skipped routing structure, a wire adjustment mechanism was designed to decouple at joint 2. The designed bionic waist joint has the same DOF and the approximate joint ROM as human, so it can well simulate the motion of human waist. Finally, a rotation angle verification experiment was conducted. It was found that the mechanism met the design requirements and could realize the coupled tendon-driven mechanism.

REFERENCES

[1] Statistics Bureau, "Statistical Handbook of Japan 2020," 2020.

[2] C. Hamou, N. R Shah, L. DiPonio, C. M Curtin, "Pinch and elbow extension restoration in people with tetraplegia: a systematic review of the literature, " *J Hand Surg Am.*, vol. 34, no. 4, pp. 692-701, Apr. 2009.

[3] S. Shirafuji, S. Ikemoto, and K. Hosoda, "Development of a tendon-driven robotic finger for an anthropomorphic robotic hand," *Int. J. Rob. Res.*, vol. 33, no. 5, pp. 677–693, 2014.

[4] Y. Kim, "Anthropomorphic Low-Inertia High-Stiffness Manipulator for High-Speed Safe Interaction," in *IEEE Transactions on Robotics*, vol. 33, no. 6, pp. 1358–1374, Dec. 2017.

[5] K. A. Wyrobek, E. H. Berger, H. F. M. Van Der Loos, and J. K. Salisbury, "Towards a Personal Robotics Development Platform: Rationale and Design of an Intrinsically Safe Personal Robot," in *2008 IEEE International Conference on Robotics and Automation*, pp. 2165–2170, 2008.

[6] A. M. M. Orner *et al.*, "Development of a humanoid robot having 2-DQF waist and 2-DOF trunk," in *5th IEEE-RAS International Conference on Humanoid Robots*, pp. 333–338, 2005.

[7] S. Yun, J. Seo, J. Yoon, H. Song, Y. Kim, and Y. Kim, "3 - DOF Gravity Compensation Mechanism for Robot Waists with the Variations of Center of Mass *," in *2019 IEEE/RSJ International Conference on Intelligent Robots and Systems (IROS)*, pp. 3565–3570, 2019.

[8] W. M. Hinojosa, N. G. Tsagarakis, G. Metta, F. Becchi, G. Sandini, and D. G. Caldwell, "Performance Assessment of a 3 DOF Differential Based Waist joint for the " iCub " Baby Humanoid Robot," in *15th IEEE International Symposium on Robot and Human Interactive Communication*, pp. 195-201, 2006.

[9] W. Li et al., "Modularization of 2- and 3-DoF Coupled Tendon-Driven Joints," in *IEEE Transactions on Robotics*, vol. 37, no. 3, pp. 905-917, Jun. 2020.

[10] H. M. Clarkson, Musculoskeletal Assessment: Joint Range of Motion and Manual Muscle Strength, Wolters Kluwer, 2013.